PHYSICAL REVIEW A VOLUME 42, NUMBER 4 15 AUGUST 1990

Spiral-wave dynamics in a simple model of excitable media: The transition from simple to compound rotation

Dwight Barkley
Applied and Computational Mathematics, Princeton University, Princeton, New Jersey 08544

Mark Kness and Laurette S. Tuckerman
Center for Nonlinear Dynamics and Department of Mathematics, University of Texas, Austin, Texas 78712

(Received 14 May 1990)

Two-dimensional reaction-diffusion equations with simple reaction kinetics are used to study the dynamics of spiral waves in excitable media. Detailed numerical results are presented for the transition from simple (periodic) rotation to compound (quasiperiodic) rotation of spiral waves. It is shown that this transition occurs via a supercritical Hopf bifurcation and that there is no frequency locking within the quasiperiodic regime.

While pattern formation in reaction-diffusion systems has been of interest for many years,[1] only recently have experiments been conducted in spatially extended systems for which the decay to thermodynamic equilibrium is prevented by the continuous flow of fresh reactants.[2] In these experiments, the spatiotemporal patterns that arise from the interplay of reaction and diffusion exist as truly asymptotic states. Moreover, well-defined control parameters exist experimentally and it is possible to investigate transitions between different dynamical states.

Of current interest is an instability exhibited by spiral waves in two-dimensional reaction-diffusion systems with excitable chemical kinetics.[3-7] The instability is as follows: for some values of the system parameters, spiral waves undergo rigid, periodic rotation. As a control parameter is varied, the periodic rotation gives way to two-frequency, quasiperiodic rotation. These two states of spiral-wave rotation have been called simple and compound rotation,[8] respectively. While there is some evidence to suggest that the transition from simple to compound rotation occurs via a Hopf bifurcation,[3-7] neither experiment nor simulation has, thus far, been conclusive as to the nature of this bifurcation. Here we use a simple model of an excitable chemical reaction as the basis for investigating the transition to compound rotation.

The model we consider consists of two chemical species, u and v, which obey the reaction-diffusion equations

$$\frac{\partial u}{\partial t}=f(u,v)+\nabla^2 u,\quad \frac{\partial v}{\partial t}=g(u,v)+\nabla^2 v\,. \tag{1}$$

The local reaction kinetics are given by

$$f(u,v)=\frac{1}{\epsilon}u(1-u)[u-u_{\rm th}(v)],\quad g(u,v)=u-v\,, \tag{2}$$

where $u_{\rm th}(v)=(v+b)/a$, and a, b, and ϵ are parameters. The parameter ϵ is typically small so that the time scale of u is much faster than that of v. The local kinetics, i.e., the dynamics in the absence of spatial derivatives, has a stable but excitable fixed point at the intersection of the nullclines $f(u,v)=0$ and $g(u,v)=0$ (see Fig. 1). Models of this kind have long been used to study excitable systems.[3-5,9,10]

The advantage of our model kinetics is that the reaction terms can be time stepped with little computational effort. At any fixed spatial location, the system spends almost all its time within a small "boundary layer" near the left branch of the u nullcline (Fig. 1). Equivalently, at any instant in time, almost all spatial points are within this boundary layer (see Fig. 2). Thus, efficient time stepping of the kinetics is obtained with the algorithm

$$\begin{aligned}&\text{if } u^n<\delta, \text{ then}\\ &\quad u^{n+1}=0\,,\\ &\quad v^{n+1}=(1-\Delta t)v^n\,,\\ &\text{otherwise,}\\ &\quad u_{\rm th}=(v^n+b)/a\,,\\ &\quad v^{n+1}=v^n+\Delta t(u^n-v^n)\,,\\ &\quad u^{n+1}=u^n+(\Delta t/\epsilon)u^n(1-u^n)(u^n-u_{\rm th})\,,\end{aligned} \tag{3}$$

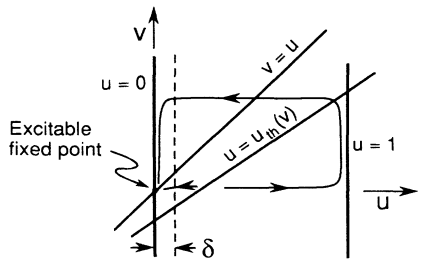

FIG. 1. Illustration of the local reaction kinetics. The axes are the concentrations of the chemical species u and v. Shown are the system nullclines: the v nullcline, $g(u,v)=0$, is the line $v=u$, and the u nullcline, $f(u,v)=0$, consists of three lines, $u=0$, $u=1$, and $u=u_{\rm th}(v)=(v+b)/a$. An excitable fixed point sits at the origin where the u and v nullclines intersect. $u_{\rm th}$ is the excitability threshold for the fixed point. Initial conditions near the fixed point and to the left of the threshold decay directly to the fixed point. Initial conditions to the right of the threshold undergo a large excursion before returning to the fixed point. δ denotes a small "boundary layer" within which the system spends most of its time.

where u^n and v^n are the value of species u and v at the nth time step (as some point in the spatial domain), Δt is the time step, and δ is the size of the boundary layer. Very little error results from setting $u^{n+1}=0$ within the boundary layer, and yet, the advantage gained is that almost every step of our model kinetic requires just one conditional evaluation and one floating-point multiplication.

The simulation of (1) is as follows. The Laplacians are evaluated by finite differences on a regular square grid using the nine-point formula[11]

$$6h^2\nabla^2 u_{ij}=\sum_{r,s}A_{rs}u_{i+r,j+s}-20u_{ij}\ ,$$

and similarly for $\nabla^2 v_{ij}$, where u_{ij} is the value of u at grid point (i,j), h is the grid spacing, and where $A_{rs}=4$ for the four nearest neighbors, $A_{rs}=1$ for the four diagonal next-nearest neighbors, and $A_{rs}=0$ otherwise. This choice of A_{rs} gives a rotationally invariant Laplacian to $O(h^4)$. No-flux boundary conditions are imposed on the domain boundary. The diffusion terms are time stepped by the explicit Euler method and the reaction time terms are stepped by (3). Operator splitting is used: the reaction and diffusion terms are updated in alternation. There are seven parameters for the problem: the four "physical parameters" a, b, ϵ, and L (L^2 being the area of the square domain), and three "numerical parameters" Δt, δ, and N, where N^2 is the number of spatial grid points.

Figure 2 shows a spiral wave obtained from our simulations. The wave is executing compound rotation: the wave rotates, and as it does, its shape changes near the tip of the spiral. Figure 3(a) shows the path taken by the spiral tip over the course of four wave rotations. (Despite its appearance, the tip path is not a closed curve and after a long time the path covers an annular region.) We take the spiral tip to be the intersection of the two contours $u=\frac{1}{2}$ and $f(u=\frac{1}{2},v)=0$, where f is given in (2). Other definitions have been used,[4,5,12] and while they all give approximately the same tip, we have found that our definition best serves our purposes because it is the least sensitive to the effects of spatial discretization.

Tip paths are shown in Fig. 3 for three values of the parameter a. Shown are paths both in the "laboratory" frame (coordinates stationary with respect to the domain boundary) and in a rotating coordinate system (x',y'). The situation is as follows. Near the center of the grid, the system is not sensitive to the square boundaries of the domain, and hence as regards tip motion, the problem has an approximate rotational symmetry. The simple periodic rotations are, to a good approximation, rotating waves[13] and the corresponding paths are circles in the laboratory frame. The compound rotations are (approximately) modulated waves, and hence there is a rigidly rotating reference frame (x',y') in which they are seen as periodic.[13] In the rotating frame these tip paths are not circular, and hence in the laboratory frame, *the paths corresponding to compound rotations are not epicycloids.* This is to be expected in that no symmetry in the problem dictates that the paths in the rotating frame be circular. Near onset, paths in the rotating frame will generically be elliptical.

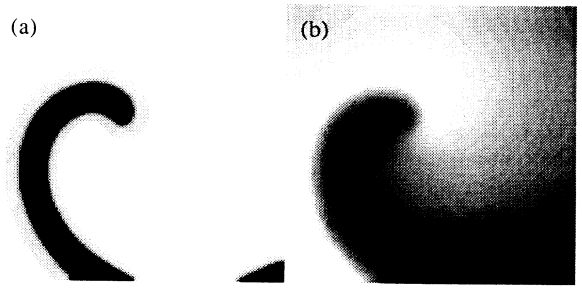

FIG. 2. Spiral wave from simulation. (a) and (b) are gray-scale contours of the species u and v, respectively. The wave is executing compound rotation. The tip path is shown in Fig. 3(a). Throughout the white region in (a), u is within the boundary layer illustrated in Fig. 1. The parameters for the simulation are $a=0.3$, $b=0.01$, $\epsilon=2.5\times10^{-3}$, $L=15$, $\Delta t=1.39\times10^{-3}$, $N=181$, and $\delta=10^{-5}$.

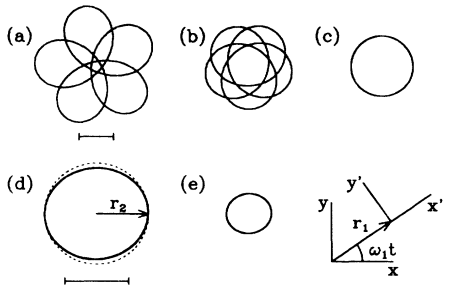

FIG. 3. Paths of the spiral tip. (a)–(c) are paths in the "laboratory" frame. (a) and (b) correspond to compound rotations and (c) to simple rotation of the spiral wave. (a) and (b) are not exactly closed curves (see Fig. 5). The parameter values are the same as in Fig. 2 except that (a) $a=0.3$, (b) $a=0.309$, and (c) $a=0.318$. (d)–(e) are the paths of (a) and (b) as seen in the rotating frame. The relationship between the laboratory frame (x,y) and the rotating frame (x',y') is illustrated at the lower right-hand side. At each parameter value, the (x,y) coordinates are centered with respect to the tip path. The angular velocity ω_1 is the mean angular velocity of the tip in the (x,y) system, and the radius r_1 is the median radius of the tip in the (x,y) system. The length scales of plots (a)–(c) are the same, as are the length scales of plots (d) and (e). Line segments denote unit length. The path in (c) is very nearly a circle and is seen as a point in the (x',y') system. The dashed circle in (d) is added to emphasize that in the rotating frame the paths of compound rotations are not circles.

To provide evidence that a supercritical Hopf bifurcation is responsible for the transition indicated in Fig. 3, we have computed the decay rates to the simple rotations on one side of the transition, and we have computed the amplitude ratios of the two modes of compound rotations on the other side of the transition (see Fig. 4). The amplitude r_1 of the primary mode is the median radius in the laboratory frame (Fig. 3). The amplitude ("radius") of the secondary mode r_2 is defined to be the maximum value of x' for the path in the rotating frame. For example, the dashed circle in Fig. 3(d) has radius r_2. Decay rates have been obtained by perturbing the spiral waves from the circular orbits and fitting the asymptotic decay back to circles $r_2(t_n)=\exp(-\lambda t_n)$, where $r_2(t_n)$ is the nth relative maximum of x' (at time t_n), and λ is the decay rate (i.e.,

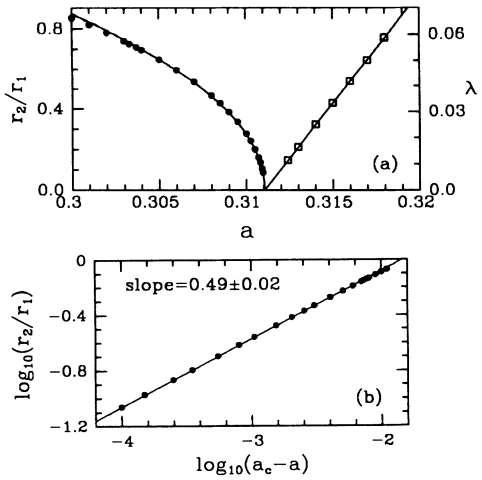

FIG. 4. (a) Amplitude ratios r_2/r_1 (points) for compound rotations and decay rates λ (squares) to simple rotations, as a function of the parameter a. Linear extrapolation to zero decay rate gives the bifurcation point as $a_c = 0.311\,05 \pm (2\times10^{-5})$. (b) log-log plot of the amplitude ratio vs distance from the bifurcation point. The best-fit line to the 14 points closest to the transition gives an exponent of 0.49 ± 0.02, where the uncertainty derives from the uncertainty in a_c. The curve with best-fit exponent is shown in (a). A supercritical Hopf bifurcation is clearly indicated by the data.

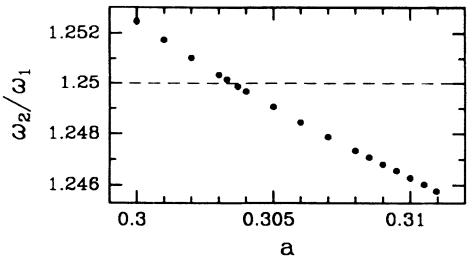

FIG. 5. Frequency ratio ω_2/ω_1 for compound rotations as a function of the parameter a. The frequency ratio $\frac{5}{4}$ corresponds to a closed five-lobed tip path. There is no evidence of frequency locking. The frequency ratio crosses the value $\frac{5}{4}$ transversely and any mode locking at this low-order frequency ratio must occur on an interval smaller than 0.1% in the parameter a.

minus the real part of the bifurcating eigenvalue).

The amplitude of the secondary mode grows from zero at the same point, a_c, where the decay rate goes through zero. Near the bifurcation point, the growth of the secondary mode is given by a power law with exponent $\sim\frac{1}{2}$. The frequencies of both modes behave regularly through the transition (not shown, but see Fig. 5). These observations provide the first conclusive evidence that the transition from simple to compound rotation occurs via a supercritical Hopf bifurcation.

The frequency ratio in the quasiperiodic regime is shown in Fig. 5. The primary frequency ω_1 is the rotational velocity of the (x',y') coordinate system (Fig. 3). We take the secondary frequency to be $\omega_2 = 2\pi/\tau$, where τ is the period as seen in the rotating frame (x',y'). The secondary frequency has been defined differently elsewhere;[4,7,14] our choice of ω_2 is standard for modulated waves.[13] As in experiment,[7] there is no evidence of frequency locking between the primary and secondary modes.[15] Most notably, there is no indication of entrainment as the frequency ratio crosses $\frac{5}{4}$. At such a low-order frequency ratio, any tendency which the system might have to mode lock should be most pronounced.[16] It is clear from Fig. 5 that the degree of frequency locking in compound rotation is negligible.

We have presented a numerical study of the transition from simple to compound rotation of spiral waves with a view to characterizing the bifurcation underlying this instability. By measuring not only the amplitude ratios for compound rotations, but also the decay rates to simple rotations, we have obtained the first definitive evidence that a supercritical Hopf bifurcation gives rise to compound rotations. In addition, we have shown that the two frequencies of compound rotation do not entrain. We note that recently Kessler and Levine[17] have shown that planar traveling waves can also undergo a Hopf bifurcation. While at present it is not possible to relate directly the bifurcation of planar waves to the Hopf bifurcation examined here, heuristic arguments suggest a connection between the two bifurcations[17] and this might be exploited in the future to provide an analytic treatment of the spiral-wave instability.

We have benefited greatly from discussions with A. Arneodo, B. Dornblaser, W. D. McCormick, W. Reynolds, G. Skinner, H. L. Swinney, and G. Zanetti. We are grateful to H. C. Othmer for communicating results prior to publication. D.B. is supported by DARPA Grant No. N00014-86-K-0759 and NSF Grant No. ECS-8945600. M.K. and L.S.T. are partially supported by NSR Grant No. DMS-8901767.

[1]A. M. Turing, Philos. Trans. R. Soc. London, Ser. **B237**, 37 (1952); A. Zaikin and A. M. Zhabotinskii, Nature (London) **225**, 535 (1970); A. T. Winfree, Science **175**, 634 (1972); O. E. Rössler and C. Kahlert, Z. Naturforsch. **34A**, 565 (1979); K. I. Agladze, A. V. Panfilov, and A. N. Rudenko, Physica **29D**, 409 (1988); J. Ross, S. C. Müller, and C. Vidal, Science **240**, 460 (1988); J. J. Tyson and J. P. Keener, Physica **32D**, 327 (1988).

[2]See, e.g., Z. Noszticzius, W. Horsthemke, W. D. McCormick, H. L. Swinney, and W. Y. Tam, Nature (London) **329**, 619 (1987); Q. Ouyang, J. Boissonade, J. C. Roux, and P. De Kepper, Phys. Lett. A **134**, 282 (1989).

[3]V. S. Zykov, Biofizika **31**, 862 (1986).

[4]W. Jahnke, W. E. Skaggs, and A. T. Winfree, J. Phys. Chem. **93**, 740 (1989).

[5]E. Lugosi, Physica **40D**, 331 (1989).

[6]T. Plesser, S. C. Müller, and B. Hess, J. Phys. Chem. (to be published).

[7]G. S. Skinner and H. L. Swinney, Physica D (to be published).

[8]The term meander was used by A. T. Winfree [Science **181**, 937 (1973)] to describe nonrigidly rotating waves. More recently the terms compound circular motion and compound rotation have been used to describe deterministic two-frequency rotations (see Refs. 3–7).

[9]See, e.g., R. Fitzhugh, Biophys. J. **1**, 445 (1961); J. J. Tyson and P. C. Fife, J. Chem. Phys. **73**, 2224 (1980); E. Meron and P. Pelcé, Phys. Rev. Lett. **60**, 1880 (1988).

[10]It should be noted that problems can arise in our model if the system gets close to the "corners" where the diagonal segment of the u nullcline intersects the vertical segments. There are no such difficulties for the spiral waves presented here.

[11]*Handbook of Mathematical Sciences,* 6th ed. (Chemical Rubber, Boca Raton, 1987), p. 657.

[12]H. G. Othmer (private communication).

[13]D. A. Rand, Arch. Ration. Mech. Anal. **79**, 1 (1982).

[14]Our secondary frequency equals the sum of the primary and secondary frequencies in Refs. 4 and 7.

[15]This is also evident to a lesser degree in Ref. 4.

[16]V. I. Arnold, *Geometric Methods in the Theory of Ordinary Differential Equations* (Springer, New York, 1983), Chap. 6.

[17]D. A. Kessler and H. Levine, Phys. Rev. A **41**, 5418 (1990).

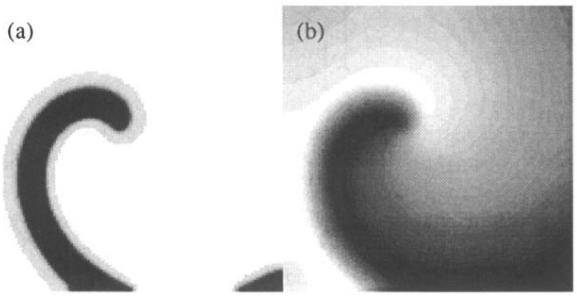

FIG. 2. Spiral wave from simulation. (a) and (b) are gray-scale contours of the species u and v, respectively. The wave is executing compound rotation. The tip path is shown in Fig. 3(a). Throughout the white region in (a), u is within the boundary layer illustrated in Fig. 1. The parameters for the simulation are $a=0.3$, $b=0.01$, $\epsilon=2.5\times10^{-3}$, $L=15$, $\Delta t=1.39\times10^{-3}$, $N=181$, and $\delta=10^{-5}$.